ACS APPLIED MATERIALS & INTERFACES

Research Article

www.acsami.org

Rethinking Band Bending at the P3HT–TiO_2 Interface

Andrew J. Haring, Spencer R. Ahrenholtz, and Amanda J. Morris*

Department of Chemistry, Virginia Tech, Blacksburg, Virginia 24061, United States

Supporting Information

ABSTRACT: The advancement of solar cell technology necessitates a detailed understanding of material heterojunctions and their interfacial properties. In hybrid bulk heterojunction solar cells (HBHJs), light-absorbing conjugated polymers are often interfaced with films of nanostructured TiO_2 as a cheaper alternative to conventional inorganic solar cells. The mechanism of photovoltaic action requires photoelectrons in the polymer to transfer into the TiO_2, and therefore, polymers are designed with lowest unoccupied molecular orbital (LUMO) levels higher in energy than the conduction band of TiO_2 for thermodynamically favorable electron transfer. Currently, the energy level values used to guide solar cell design are referenced from the separated materials, neglecting the fact that upon heterojunction formation material energetics are altered. With spectroelectrochemistry, we discovered that spontaneous charge transfer occurs upon heterojunction formation between poly(3-hexylthiophene) (P3HT) and nanocrystalline TiO_2. It was determined that deep trap states (0.5 eV below the conduction band of TiO_2) accept electrons from P3HT and form hole polarons in the polymer. This equilibrium charge separation alters energetics through the formation of interfacial dipoles and results in band bending that inhibits desired photoelectron injection into TiO_2, limiting HBHJ solar cell performance. X-ray photoelectron spectroscopic studies quantified the resultant vacuum level offset to be 0.8 eV. Further spectroelectrochemical studies indicate that 0.1 eV of this offset occurs in TiO_2, whereas the balance occurs in P3HT. New guidelines for improved photocurrent are proposed by tuning the energetics of the heterojunction to reverse the direction of the interfacial dipole, enhancing photoelectron injection.

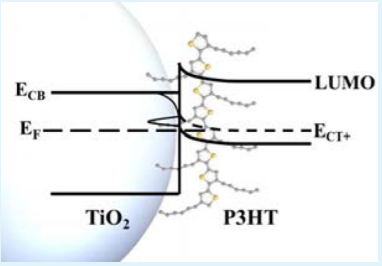

KEYWORDS: *P3HT, polymer, TiO_2, heterojunction, photovoltaic, polaron*

INTRODUCTION

Next generation solar cells include low-cost, thin hybrid bulk heterojunction solar cells (HBHJs), where nanostructured metal oxide semiconductors act as the acceptor for conjugated polymer light absorbers.[1,2] Nanostructured metal oxides provide high surface area for charge injection from polymers, as well as directed electron transport to the electrode. Although high photocurrent can potentially be collected, only efficiencies as high as 3% have been obtained.[2] Further investigations into the optimization of the organic–inorganic interface are required to realize the full potential of HBHJs.[3−5]

The alignment of donor and acceptor energy levels for thermodynamically favorable photoelectron transfer is paramount for HBHJ device function.[6] Upon illumination, photoelectrons in the lowest unoccupied molecular orbital (LUMO) of the light absorbing polymer are electrostatically bound to the hole created in the highest occupied molecular orbital (HOMO) by 0.1−0.3 eV.[6] The LUMO energy level, E_{LUMO}, must be situated at least 0.3 eV above the energy of the conduction band of TiO_2, E_{CB}, for efficient electron transfer.[7−9] At the same time, a larger energy gap between E_{CB} and the polymer HOMO energy level, E_{HOMO}, allows for greater photovoltage. However, the polymer's optical energy gap must also be optimized to absorb sufficient sunlight (~1.6−2.0 eV). Therefore, ideal materials have a $\Delta E_{LUMO-CB} \geq 0.3$ eV while maintaining high $\Delta E_{CB-HOMO}$ (≥1.3 eV). This ideal energy alignment imposes requirements on both materials and provides general guidelines for synthetically designing light-absorbing polymers. Thus, synthesizing polymers with different energetic properties has garnered much attention in pursuit of HBHJs delivering high power conversion efficiencies.[3−5,10,11]

However, forming a heterojunction alters materials' energetics, complicating the applicability of these general guidelines.[12] For example, at inorganic semiconductor p–n junctions and some metal–metal junctions, two materials with different Fermi levels (E_F) are brought together, leading to charge transfer and the generation of an interfacial dipole that shifts energy levels at the interface (vacuum level offset).[13,14] At thermodynamic equilibrium, the Fermi level (chemical potential of electrons) must be constant throughout the semiconductor junction.[13] Before equilibration, when two semiconductors with different Fermi levels come into electrical contact, an initial chemical potential gradient at the interface exists, which results in spontaneous electron transfer down the gradient, from the semiconductor with higher E_F to the semiconductor with lower E_F.[13] Thermodynamic equilibrium is attained when the new charge distribution generates an electric field, extending 10−1000 nm to either side of the interface (interfacial dipole), that prevents further electron transfer.[13] Since the conduction and valence bands represent the potential energy of electronic states in the region of the electric field, they bend downward or upward in energy.

Received: January 6, 2014
Accepted: February 26, 2014
Published: February 26, 2014

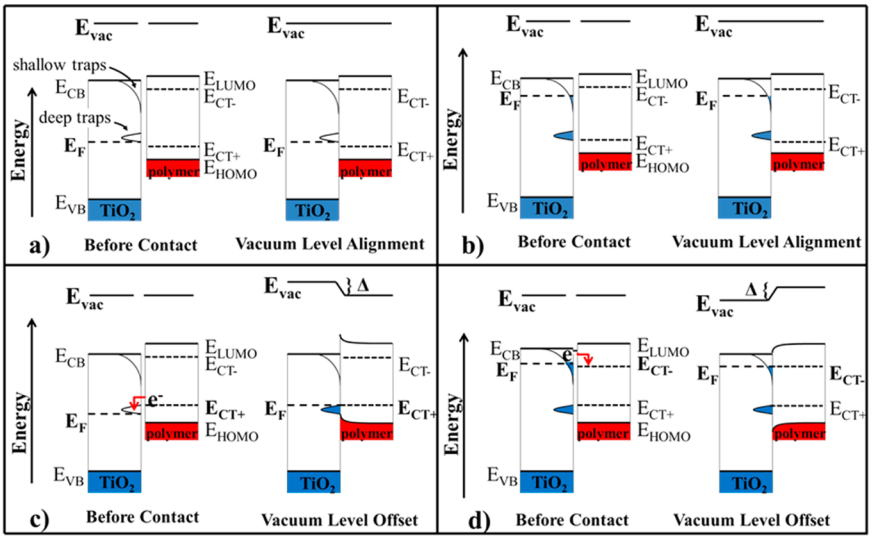

Figure 1. Band diagrams illustrating the possible energy alignment regimes in polymer−TiO_2 heterojunctions. The TiO_2 Fermi level between E_{CT-} and E_{CT+} prevents charge transfer and leads to vacuum level alignment, whether E_F in TiO_2 is below deep traps (a) or above deep traps (b). The TiO_2 Fermi level below E_{CT+} (c) or above E_{CT-} (d) results in charge transfer and vacuum level offset. The portion of the vacuum level offset occurring in mesoporous TiO_2 is homogeneous throughout the film because band bending is limited by the nanoparticle size (15−20 nm), vide infra.

Charge transfer and band bending can also occur at the interface of polymers with nanocrystalline TiO_2, but the model of inorganic semiconductors cannot be directly applied.[15−18] Whereas energy level alignment is determined by the initial Fermi level gradient at the interface for semiconductor junctions, it is determined by the TiO_2 Fermi level and the polymer's polaronic energy levels for TiO_2−polymer junctions.[19,20] Adding excess electrons or holes to organic materials distorts the molecular geometry, and the excess charge couples with the relaxed geometry, creating polarons with energies in the HOMO−LUMO gap, discussed in more detail below.[21] Charge transfer and band bending occurs when polaron formation is thermodynamically favorable (vacuum level offset).[19,20] Forming hole polarons in the polymer leads to downward band bending, which inhibits photoelectron injection into the TiO_2.[22] In contrast, forming electron polarons in the polymer improves photoelectron injection into the TiO_2.

Herein, spontaneous charge transfer was detected in heterojunctions of poly(3-hexylthiophene) (P3HT) and nanocrystalline TiO_2, which generates a vacuum level offset. Spectroelectrochemical studies show that TiO_2 donates holes into P3HT upon forming the heterojunction. Charge redistribution between the hole polaron level in P3HT (E_{CT+}) and the Fermi level of TiO_2 creates an interfacial dipole that bends the P3HT energy levels downward (lower energy away from the interface). Thus, photoelectron injection is inhibited in HBHJ solar cells based on the P3HT−TiO_2 heterojunction. Additionally, raising the TiO_2 Fermi level above E_{CT+} prevented charge transfer and led to vacuum level alignment, lending further support to the importance of the polaron levels proposed by Salaneck et al.[19] By controlling the direction and magnitude of band bending, solar cells with improved photocurrent and power conversion efficiencies can be designed. Optimized polymers should be designed with electron polaron levels (E_{CT-}) lower than the Fermi level of TiO_2, allowing for electron polaron formation and upward band bending that should increase solar cell photocurrent.

EXPERIMENTAL METHODS

HPLC-grade acetonitrile (99.9%) from Spectrum Chemical was distilled once, and tetrabutylammonium hexafluorophosphate ($TBAPF_6$, >98.0%) from Fluka Analytical was recrystallized four times from ethyl acetate prior to use. 1,2-Dichlorobenzene, tetrahydrothiophene (THT, 99%), and thiophene (>99%) from Sigma Aldrich, 2,5-dimethylthiophene (DMT, >98%) from Alfa Aesar, and poly(3-hexylthiophene-2,5-diyl) (P3HT, 91−94% regioregularity) from Rieke Metals were used without further purification.

Electrode Preparation. Fluorine-doped tin oxide-coated glass (FTO-glass, 12−14 Ω cm^{-2}) was purchased from Hartford Glass Co. for transparent-conducting electrodes. FTO-glass slides (5 × 1 × 0.23 cm) were ultrasonicated for 15 min in aqueous Alconox detergent and rinsed with deionized water. The sonication/rinsing cycle was repeated with ethanol and acetone, respectively. After air-drying, transparent mesoporous TiO_2 films (1 cm^2) were synthesized by doctor-blading Solaronix T/SP paste (100% anatase, 15−20 nm) onto the cleaned FTO-glass. The films were heated at 450 °C for 30 min after a 7°/min ramp. Reduced-TiO_{2-x} films were prepared by further annealing TiO_2 under vacuum (10^{-5} Torr) for 2 h. While still warm (~80 °C), the films were soaked in vials of 1 mg/mL P3HT in 1,2-dichlorobenzene or 0.1 M thiophene, THT, or DMT in acetonitrile at 60 °C for 6 h to sensitize the films. Hereafter, sensitized films are referred to as P3HT−TiO_2, thiophene−TiO_2, THT−TiO_2, DMT−TiO_2, or unfunctionalized-TiO_2, respectively. Prior to use, the films were air-dried and rinsed with neat acetonitrile.

Spectroelectrochemistry. The working electrodes, as prepared above, were used in a ground-glass joint quartz cuvette (Quark) with a Pt mesh counter electrode and an Ag/AgCl saturated KCl reference electrode, calibrated with $K_4[Fe(CN)_6]$ from Fisher Scientific. All electrochemistry experiments were performed with 0.1 M $TBAPF_6$ in acetonitrile as the electrolyte. The electrochemical cells were sealed and purged with argon for 20 min to remove dissolved oxygen. Potentials were applied with a BASi Epsilon potentiostat while monitoring the absorbance of the working electrodes with a Cary 5000 UV−vis-NIR spectrophotometer. The molar absorptivity at 950 nm of $TiO_2(e^-)$s (electrons occupying shallow traps in TiO_2) was determined by comparing their absorbance at 800 and 950 nm, knowing that ε = 1300 M^{-1} cm^{-1} at 800 nm.[23]

X-ray Photoelectron Spectroscopy (XPS). XPS was conducted using a PHI 5300 spectrometer with a Perkin-Elmer Dual Anode X-ray source operating with magnesium radiation with monochromatic Mg Kα radiation (hν 1253.6 eV) at 13 kV and 250 W and a pass energy of

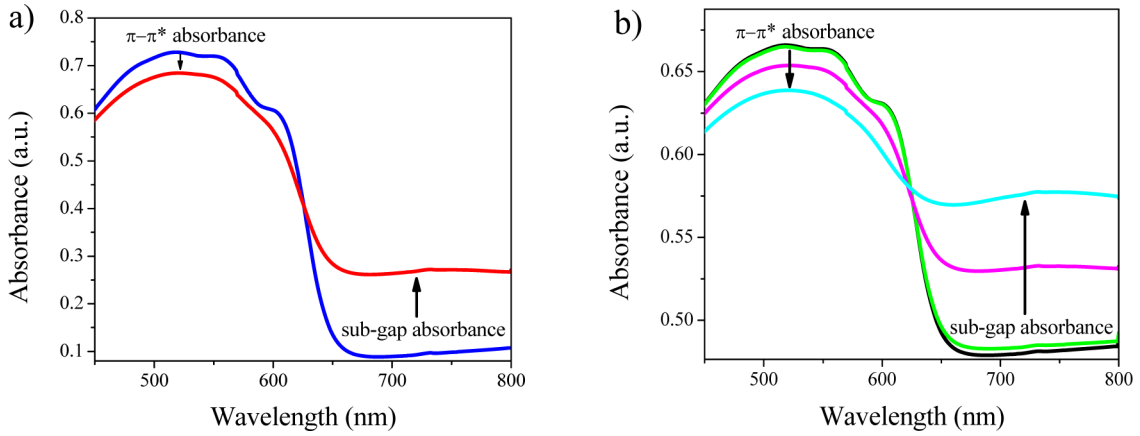

Figure 2. Spectroelectrochemistry of P3HT−TiO_2 and P3HT alone. (a) Oxidized P3HT−TiO_2 with no applied potential (red) and neutral P3HT−TiO_2 after applying −0.5 V (blue). (b) Neutral P3HT (black) and oxidized P3HT after applying +0.2 V vs Ag/AgCl (green), +0.4 V (magenta), and +0.6 V (cyan).

17.9 eV. Emitted photoelectrons were detected by a hemispherical analyzer, and the operating pressure in the sampling chamber was below 10^{-7} Torr. The instrument work function was calibrated to adventitious carbon (C 1s peak at 284.8 eV) and an external Ag sample (Ag $3d_{5/2}$ peak at 383.3 eV).[24] The spectral scanning range for the valence region was 0−35 eV, with a step size of 0.125 eV and 10 sweeps averaged.

RESULTS AND DISCUSSION

Energy Level Alignment Regimes. Energy level alignment at polymer−TiO_2 heterojunctions is characterized by vacuum level alignment or vacuum level offset. In heterojunctions where charge transfer is thermodynamically unfavorable, upon interfacing the materials, the energy levels of the separated materials are maintained at the interface and their vacuum levels align. In materials where spontaneous charge transfer occurs, an interfacial dipole forms that offsets the respective vacuum levels and bends energy levels near the interface. For vacuum level offset to occur in the polymer−TiO_2 heterojunction, charge transfer into unoccupied states must be thermodynamically favorable.

The relevant charge transfer states in the polymer are not the HOMO and LUMO, but the energy of electron or hole polarons, E_{CT-} and E_{CT+}, respectively.[19] When organic materials are ionized by electron or hole transfer, the molecular geometry distorts near the excess charge.[21] The charge couples with the local molecular distortion and forms a polaron, with lower energy than an excess charge on the undistorted molecule. Charge coupling with relaxed molecular distortions creates electron or hole polaronic states that lie within the HOMO−LUMO gap. For example, electron transfer from the HOMO of neutral P3HT transforms aromatic thiophene units into their quinoid-like counterparts, and the resulting hole polarons are localized to 5−15 thiophene units, positioned 0.2−1 eV above the HOMO energy level.[15,20,25] The presence of hole polarons in films of oxidized $P3HT^{\bullet+}$ and similar conjugated polymers can be detected by visible light absorption changes, in addition to Raman and electron paramagnetic resonance spectroscopies (EPR).[26−29]

Energy level alignment in the case of TiO_2 and polymers depends on the possibility of charge transfer between TiO_2 and the polaronic levels. If the Fermi level of TiO_2 is situated in-between E_{CT-} and E_{CT+}, charge transfer between the materials is thermodynamically unfavorable and will not contribute to interfacial dipoles.[18] Therefore, the energy levels will align according to vacuum level alignment, Figure 1a,b. If the Fermi level in TiO_2 is situated below E_{CT+}, holes will transfer to the polymer, creating hole polarons, Figure 1c. The resultant interfacial dipole will bend the bands in the polymer downward, inhibiting photoelectron injection. If the Fermi level is situated above E_{CT-}, electrons will transfer to the polymer, creating electron polarons, Figure 1d. In this case, the interfacial dipole will bend the bands in the polymer upward, improving photoelectron injection and charge separation.

Charge Transfer between P3HT and TiO_2. Spectroelectrochemistry was utilized to investigate spontaneous charge transfer at P3HT−TiO_2 heterojunctions. Upon forming the P3HT−TiO_2 heterojunction, the P3HT absorbance spectrum exhibits two features different than films of P3HT alone. P3HT on TiO_2 displays reduced π−π^* absorbance and increased subgap absorbance as compared to P3HT on FTO-glass. After applying −0.5 V vs Ag/AgCl, the ground state absorbance is observed in P3HT−TiO_2, i.e., full π−π^* absorbance, Figure 2a.

The spectroelectrochemical response of P3HT films on FTO-glass was studied to determine the absorbance spectra of the neutral and oxidized states of P3HT. The onset of P3HT oxidation occurs at +0.2 V vs Ag/AgCl (0.1 M $TBAPF_6$ in MeCN), in accord with the onset of absorbance changes. Due to electronic transitions within the HOMO−LUMO gap, formation of hole polarons in $P3HT^{\bullet+}$ leads to increased subgap absorbance of near-infrared light and a concomitant bleach of ground state absorbance from π−π^* transitions in neutral P3HT, Figure 2b (black).[26] Unlike P3HT−TiO_2, application of −0.5 V did not affect the absorbance spectrum of P3HT alone, Figure S1a, Supporting Information.

Spectroelectrochemistry of P3HT−TiO_2 heterojunctions showed features consistent with P3HT oxidation, i.e., increased near-infrared absorbance and decreased absorbance around 500 nm. Applying reductive potentials to the heterojunction leads to an increase in absorbance from π−π^* transitions and a decrease in subgap absorbance, Figure 2a (blue). Fresh P3HT films on FTO-glass display their fully neutral absorbance and are not affected by application of potentials <0.2 V vs Ag/AgCl. In contrast, P3HT on TiO_2 is spontaneously oxidized and application of reductive potentials is necessary to observe the fully neutral absorbance, Figure 2a (blue). Therefore, upon making the heterojunction, electron transfer from P3HT into

mesoporous TiO_2 films is spontaneous and forms hole polarons in P3HT.

Electron transfer is energetically favorable if unoccupied states in the TiO_2 band gap are located below the hole polaron energy level, E_{CT+}. Oxygen vacancies in TiO_2 create deep traps ~0.5−1 eV below the conduction band that can accept electrons, assuming the traps are partially unoccupied.[30] By annealing TiO_2 films in an oxygen-deficient atmosphere (450 °C, vacuum), reduced-TiO_{2-x} forms, wherein excess negative charge on Ti^{3+}sites increases the Fermi level, leading to occupied deep traps.[31,32] Unlike stoichiometric TiO_2, the higher Fermi level in reduced-TiO_{2-x} does not allow spontaneous electron transfer from P3HT, Figure S1b, Supporting Information. In this case, P3HT remains neutral, evidenced by an absorbance spectrum unaffected by applying reductive potentials. Reduction of TiO_2 and the resultant increase in E_F above E_{CT+} precludes favorable charge transfer, as in Figure 1b. Preventing oxidation by increasing the Fermi level to form reduced-TiO_{2-x} corroborates the assignment of P3HT oxidation to charge transfer, rather than chemical doping by atmospheric O_2 and ambient UV radiation catalyzed by the TiO_2 surface.[33−36] Additionally, P3HT films alone were not significantly oxidized by ambient conditions in the experimental time frame, Figure S1b, Supporting Information.

For the first time, charge transfer was detected upon making P3HT−TiO_2 heterojunctions. Absorbance features indicative of hole polarons in P3HT were created when interfacing the polymer with TiO_2. Illustrated by Figure 1c, unoccupied deep traps in TiO_2 can transfer holes forming hole polarons at the E_{CT+} level in P3HT. However, reduced-TiO_{2-x}, with a higher E_F and occupied deep traps, does not allow for the oxidative charge transfer. As discussed below, the Fermi level in TiO_2 with and without P3HT can be determined by XPS, providing additional support to the charge transfer and vacuum level offset.

Vacuum Level Offset. As in semiconductor p−n junctions, upon making heterojunctions with organic layers, charge transfer results in an interfacial dipole that offsets the respective vacuum levels, Δ, Figure 1c,d.[16] Experimentally, vacuum levels are measured by the energy required to eject electrons from bulk materials to a location near the surface of the sample, $E_{vac}(s)$, although theoretically the vacuum level is defined by the energy of free electrons infinitely far from the sample, $E_{vac}(\infty)$.[25,37] In the heterojunction, electrons near the surface feel greater affinity for the positively charged material, which has a lower $E_{vac}(s)$ than the negatively charged material, representing a vacuum level offset.[15]

Vacuum level offsets are commonly determined by photoemission spectroscopy by elucidating E_F and $E_{vac}(s)$ of the heterojunction and separated materials.[17,20,38] In XPS spectra, photoemitted electrons from the occupied valence band comprise the signal intensity near E_F (zero binding energy). In TiO_2, the valence band begins 2.0 eV below E_F, and an optical band gap of 3.17 ± 0.02 eV (Figure S2, Supporting Information) places the conduction band 1.17 eV above E_F, Figure 3 (blue). In accord with n-type materials, E_F rests closer to the conduction band, although its exact value depends on the synthetic and annealing procedure of the TiO_2.[39] Therefore, deep traps from oxygen vacancies (~0.5−1 eV below the conduction band) would be unoccupied and available to accept electrons from P3HT.[30]

Compared to 2.0 eV in bare TiO_2, the valence band in the P3HT−TiO_2 heterojunction is 2.8 eV below E_F, Figure 3 (red).

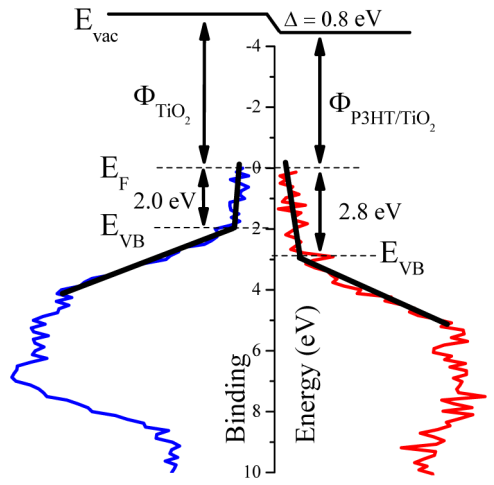

Figure 3. XPS spectra of the valence region of TiO_2 (blue) and P3HT−TiO_2 (red). E_{VB} is the valence band maximum and E_F is the Fermi level, while Δ is the vacuum level offset, 0.8 eV. The work functions Φ_{Tio_2} and Φ_{P3HT/Tio_2} and E_{vac} are not determined from the XPS data but are represented qualitatively.

After equilibrating the Fermi level in TiO_2 with E_{CT+}, charge transfer between P3HT and TiO_2 results in an interfacial dipole offsetting the vacuum levels by Δ = 0.8 eV. As in Figure 1c, the vacuum level is higher at the surface of TiO_2 with a downward gradient toward P3HT. Thus, the barrier inhibits photoelectron injection from P3HT, and the energy level alignment is unfavorable for solar cells. In accord with our XPS data, McGehee et al. used a Kelvin probe technique to determine that a 5 nm layer of P3HT on flat TiO_2 shifted its work function by 0.06 eV toward the vacuum level.[40] The difference in magnitude between these two independent measurements can be attributed to the thickness of the P3HT layer (5 nm vs 1 μm) and the accessible surface area for mesoporous vs flat TiO_2.[41]

Vacuum Level Offsets from Spectroelectrochemistry. Spectroelectrochemistry has previously been utilized to quantify shifts in TiO_2 energetics upon the formation of TiO_2/molecular interfaces.[23,42,43] Because this technique is only sensitive to absorbance changes attributed to filled TiO_2 states, it allows for isolation of the shift within the TiO_2 alone, not across the whole junction as measured with XPS. Therefore, it is used to determine the portion of the 0.8 eV vacuum level offset that occurs in TiO_2. Specifically, this technique probes the energetic position of shallow traps that lie 0−0.5 eV below the TiO_2 conduction band. Reductive potentials more negative than −0.6 V (vs Ag/AgCl) inject electrons into the shallow trap states, which are quantified by their absorbance of light >400 nm. With increasing negative potential, additional electrons are injected which corresponds to higher absorbance across the visible-near-infrared region, Figure S3, Supporting Information. In the P3HT−TiO_2 heterojunction, more negative potentials are required to achieve the same absorbance as TiO_2 alone, indicating a shift of the shallow traps toward the vacuum level, Figure 4.

From the modified Beer−Lambert law in eq 1, the molar density of electronic states, Γ, is calculated from the absorbance by electrons occupying the shallow trap states,[23]

$$\Delta A_{950\ nm} = \frac{\varepsilon(M^{-1}cm^{-1})}{1000\ cm^3/L}\Gamma\left(\frac{mol}{cm^2}\right) \quad (1)$$

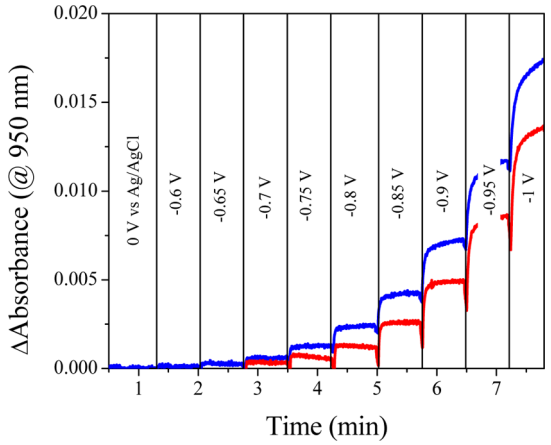

Figure 4. Absorbance of 950 nm light during potential-step spectrolelectrochemistry is due to electrons being injected into shallow traps in TiO_2 by application of the indicated potentials (blue). In P3HT−TiO_2, more negative potentials are required to achieve the same absorbance change from $TiO_2(e^-)$s (red). At these potentials, electron injection into P3HT itself does not occur, Figure S4, Supporting Information.

where the molar absorptivity of $TiO_2(e^-)$s is taken as 3300 M^{-1} cm^{-1} at 950 nm. Faraday's constant translates molar densities into the density of states, *g*, eq 2.

$$\Gamma\left(\frac{\text{mol}}{\text{cm}^2}\right) \times 96485\left(\frac{\text{C}}{\text{mol}}\right) = g\left(\frac{\text{C}}{\text{cm}^2}\right) \quad (2)$$

The energetic position of the density of states is illustrated by plotting *g* as a function of potential. Compared to bare TiO_2 in Figure 5 (blue), the onset of shallow traps is shifted toward the

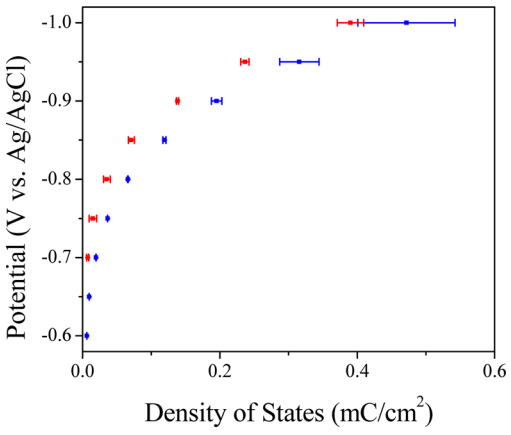

Figure 5. Spectroelectrochemistry maps the shallow traps that tail below the conduction band of TiO_2. Compared to unfunctionalized-TiO_2 (blue), P3HT shifts the potential of the density of states toward the vacuum level (red).

vacuum level from −0.6 to −0.7 V when functionalized with P3HT, Figure 5 (red). The spectroelectrochemical results were also confirmed with capacitance measurements using cyclic voltammetry, Figure S5, Supporting Information. Spectroelectrochemistry was a more sensitive technique providing a higher level of signal-to-noise.

The total vacuum level offset (0.8 eV) is composed of the energy shift that occurs in the TiO_2 layer and that which occurs in the P3HT layer. As spectroelectrochemistry indicates, the shift of TiO_2 energetics on the vacuum scale contributes 0.1 eV; band bending in the P3HT comprises the rest of the offset (0.7 eV). The 0.1 eV shift in TiO_2 is assumed to be homogeneous over each individual nanoparticle and, therefore, the entire mesoporous film, i.e., there is no observed band bending.[44−46] In contrast to planar TiO_2 films, mesoporous films cannot support an electric field because space charge gradients are limited by the radius of the nanoparticles.[47−49] However, organic materials, including P3HT, can support band bending of the measured 0.7 eV magnitude, which can extend up to 700 nm from the interface.[19,20,50]

To investigate if P3HT has structure-dependent properties contributing to vacuum level offsets other than charge transfer, molecular thiophene derivatives were used to functionalize TiO_2. By the same mechanism that interfacial dipoles created from charge transfer lead to vacuum level offsets, permanent dipoles at the surface of TiO_2 are known to shift the energetics of its states.[19,51−53] Shifts reported previously have been attributed to the direction and magnitude of dipole moments in molecular monolayers chemisorbed to planar TiO_2.[41] Therefore, small molecule thiophene mimics (tetrahydrothiophene (THT), thiophene, and dimethylthiophene (DMT)) were used to determine if dipole effects could contribute to the observed shift in TiO_2 energy levels. Whereas THT has a 1.87 D dipole moment and two lone pairs localized on the sulfur atom, thiophene has a smaller dipole moment (0.54 D) and only one lone pair. DMT has an even smaller dipole moment (0.51 D), and its sulfur atom is sterically hindered by methyl groups from attaining close contact with TiO_2 and chemisorbing through sulfur.[54] Similarly, P3HT has hexyl groups sterically hindering chemisorption through sulfur.

In accord with the shift illustrated in Figure 6a, sulfur lone pairs on THT can donate electron density toward the shallow traps in TiO_2, thus requiring higher potentials to further reduce TiO_2 by injecting electrons. However, when the sulfur atom is sterically hindered or the dipole moment is reduced, as in DMT and thiophene, respectively, there is no significant effect, Figure 6b,c. P3HT is most analogous to DMT, in which bulky groups sterically hinder the one lone pair localized on sulfur. Therefore, P3HT is not expected to significantly contribute to energy shifts through a dipole−surface interaction.

Energy Level Diagrams. From the combination of spectroelectrochemical and XPS data, energy level diagrams on the vacuum scale are generated to summarize the energy level alignment in P3HT−TiO_2 heterojunctions, Figure 7a. Electrode potentials are translated to the vacuum scale by considering that 0 V vs Ag/AgCl is −4.7 eV vs the vacuum level, Figure S6, Supporting Information.[55] The conduction band minimum is 0.5 eV above the onset of the shallow traps in TiO_2 (−4.1 eV), while deep traps extend 0.5−1 eV below the conduction band (−4.1 to −4.6 eV).[30] UV−vis measurements of the optical gap of TiO_2 places the valence band 3.17 ± 0.02 eV below the conduction band at −6.8 eV, Figure S3, Supporting Information. The onset of oxidation of P3HT (HOMO) places the Fermi level of TiO_2 below E_{CT+}, which is 0.5−0.9 eV above the HOMO.[19] Downward band bending in the polymer layer, due to the interfacial dipole, imparts a thermodynamic barrier inhibiting photoelectron injection into TiO_2, contributing to low photocurrents in HBHJs based on P3HT−TiO_2 heterojunctions.

Ideal energy level alignment would result in upward band bending and, in turn, higher photocurrent, Figure 7b. For upward band bending, the Fermi level in TiO_2 must be above

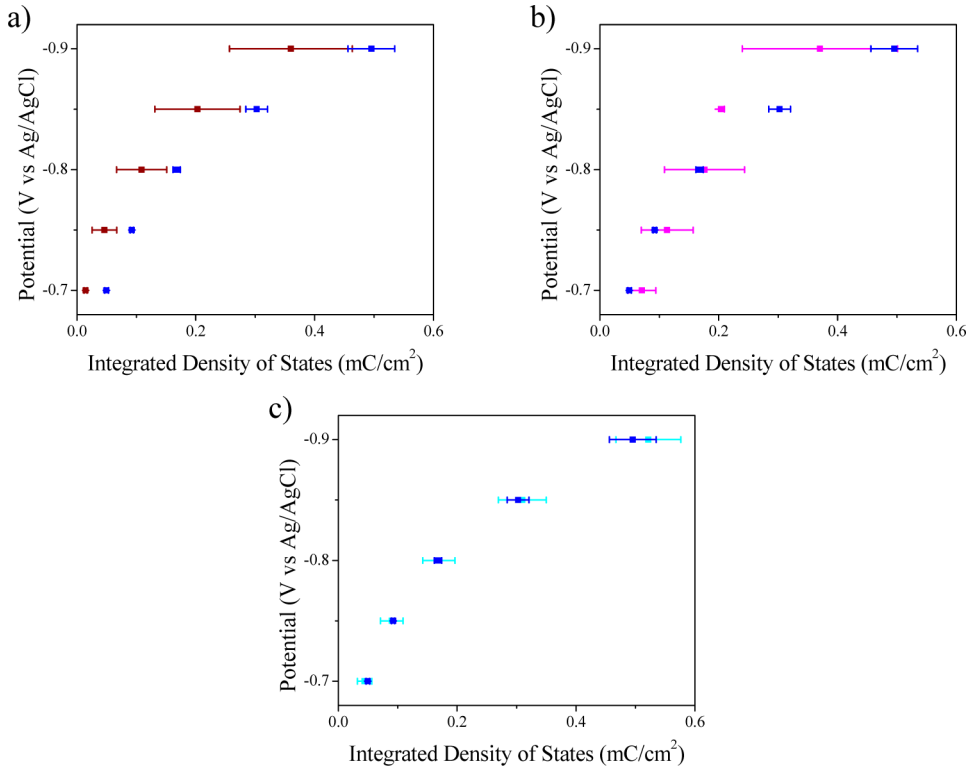

Figure 6. The shallow traps in TiO_2 films functionalized with (a) tetrahydrothiophene (dark red) are shifted toward the vacuum level compared to unfunctionalized-TiO_2 (blue). (b) 2,5-Dimethylthiophene (magenta) and (c) thiophene (cyan) do not have a significant effect.

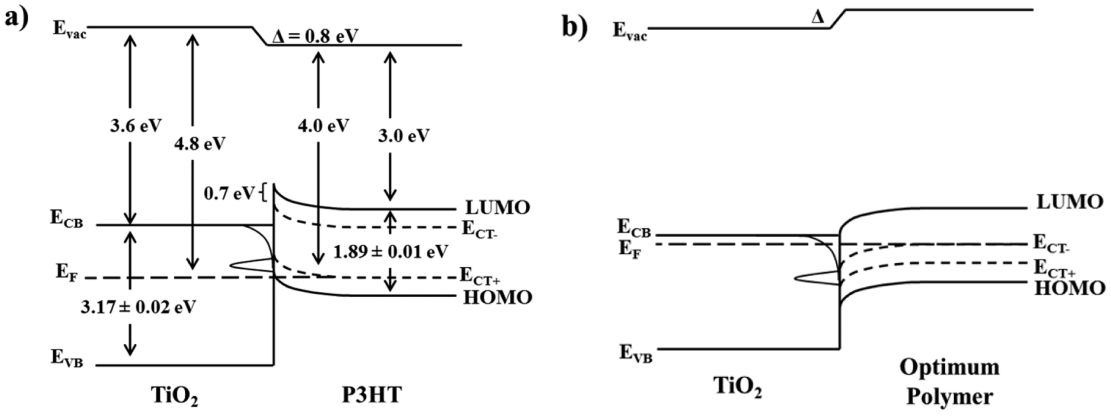

Figure 7. Energy level diagram of (a) the P3HT−TiO_2 heterojunction and (b) the optimum heterojunction. Band bending in P3HTcontributes 0.7 eV to the total 0.8 eV vacuum level offset after E_F equilibrates to the hole polaron level in P3HT, E_{CT+}. In the optimized heterojunction, E_F in TiO_2 should equilibrate in the opposite direction, to the electron polaron level, E_{CT-}.

E_{CT-} but below the LUMO level. Upon making the heterojunction, charge transfer from TiO_2 would create electron polarons in the polymer, forming an electric field in the polymer that would assist photoelectron injection. Optimized energy level alignment for efficient HBHJs requires the TiO_2 E_F to be close to E_{CB}, $\Delta E_{LUMO-CB} \geq 0.3$ eV, and $E_F > E_{CT-}$ in the separated materials.

These requirements can be met by doping TiO_2 to raise E_F and by rationally designing polymers with electron polaron levels >0.3 eV below the LUMO energy level. A possible method to raise the E_F of TiO_2 is to dope the material with Nb^{5+} forming $Nb_xTi_{1-x}O_2$.[56] Unlike other transition metals used to dope TiO_2, Nb-doping has previously been shown to maintain the overall crystal structure and E_{CB}, while raising E_F within 0.1 eV of the conduction band.[57] Likewise, doping with Ta^{5+} can raise E_F without significantly affecting the crystal structure or optical properties of TiO_2.[56,58] In contrast, even lightly doping with V^{5+} (<0.1% V/Ti ratio) significantly alters the optical properties, which would complicate the analysis of modifying E_F to optimize the polymer−TiO_2 heterojunction.[59]

To fulfill the energetic requirements for the LUMO of the optimized polymer and ensure that E_{CT-} is below E_F, the E_{CT-} of the ideal polymer needs to be lower compared to P3HT. This is possible since forming E_{CT-} in the range of 0.3−1 eV below the LUMO has been reported.[19,60] In conjugated polymers, the offset between the LUMO and E_{CT-} is partly determined by the aromaticity of the ring system, since adding an electron transforms aromatic rings to their quinoid counterparts when forming polarons. Highly aromatic homocyclic oligomers, such as pentacene, have $\Delta E_{LUMO-CT-} > 1$ eV.[60] Therefore, light-

dx.doi.org/10.1021/am500101u | ACS Appl. Mater. Interfaces 2014, 6, 4394−4401

absorbing polymers containing highly aromatic units with $\Delta E_{LUMO-CB} \geq 0.3$ eV are potential candidates to achieve upward band bending in polymer−TiO_2 heterojunctions and are the subject of continued research.

CONCLUSIONS

For the first time, charge transfer in the absence of illumination or an applied potential was detected upon making P3HT−TiO_2 heterojunctions, by spectroelectrochemistry. The resultant vacuum level offset and hole polarons in P3HT illustrate the relevance of polaronic energy levels, E_{CT+} and E_{CT-}, when designing materials for HBHJs. Due to the polaronic nature of organic materials, HBHJs cannot be modeled as a heterojunction of inorganic semiconductors, nor can vacuum level alignment be assumed to occur in all cases. Additionally, spectroelectrochemistry shows that most of the vacuum level offset is manifested as band bending in P3HT, whereas the energetics of TiO_2 are shifted by 0.1 eV throughout the mesoporous film.

Although downward band bending in P3HT−TiO_2 heterojunctions introduces a barrier toward interfacial photoelectron transport, an ideal heterojunction can be designed to impart upward band bending. To fulfill the guidelines developed above for the relative energies of the Fermi level, conduction band, and polarons, synthetic modifications, which includes TiO_2 doping and employing aromatized polymer structures, provide conditions for the thermodynamically favorable formation of electron polarons in the polymer. The resultant interfacial dipole at the ideal heterojunction assists the LUMO-E_{CB} gradient in splitting excitons into free charge carriers that produce photocurrent. By this route, the efficiency of HBHJs, currently plagued by low photocurrent (<5 mA/cm^2), can be maximized.

ASSOCIATED CONTENT

Supporting Information

Graphs of spectroelectrochemical control experiments, UV−vis spectra for determination of optical gaps, and capacitance data from cyclic voltammetry. This material is available free of charge via the Internet at http://pubs.acs.org/.

AUTHOR INFORMATION

Corresponding Author

*E-mail: ajmorris@vt.edu.

Notes

The authors declare no competing financial interest.

ACKNOWLEDGMENTS

The authors are grateful for funding provided by the Institute for Critical Technology and Applied Science and the Chemistry Department at Virginia Tech.

REFERENCES

(1) Boucle, J.; Ackermann, J. Solid-State Dye-Sensitized and Bulk Heterojunction Solar Cells Using TiO_2 and ZnO Nanostructures: Recent Progress and New Concepts at the Borderline. *Polym. Int.* **2012**, *61*, 355−373.

(2) Zhou, Y. F.; Eck, M.; Kruger, M. Bulk-Heterojunction Hybrid Solar Cells Based on Colloidal Nanocrystals and Conjugated Polymers. *Energy Environ. Sci.* **2010**, *3*, 1851−1864.

(3) Duan, C. H.; Huang, F.; Cao, Y. Recent Development of Push-Pull Conjugated Polymers for Bulk-Heterojunction Photovoltaics: Rational Design and Fine Tailoring of Molecular Structures. *J. Mater. Chem.* **2012**, *22*, 10416−10434.

(4) Wright, M.; Uddin, A. Organic-Inorganic Hybrid Solar Cells: A Comparative Review. *Sol. Energy Mater. Sol. Cells* **2012**, *107*, 87−111.

(5) Uy, R. L.; Price, S. C.; You, W. Structure-Property Optimizations in Donor Polymers Via Electronics, Substituents, and Side Chains toward High Efficiency Solar Cells. *Macromol. Rapid Commun.* **2012**, *33*, 1162−1177.

(6) Bredas, J. L.; Beljonne, D.; Coropceanu, V.; Cornil, J. Charge-Transfer and Energy-Transfer Processes in Pi-Conjugated Oligomers and Polymers: A Molecular Picture. *Chem. Rev.* **2004**, *104*, 4971−5003.

(7) Scharber, M. C.; Wuhlbacher, D.; Koppe, M.; Denk, P.; Waldauf, C.; Heeger, A. J.; Brabec, C. L. Design Rules for Donors in Bulk-Heterojunction Solar Cells - Towards 10% Energy-Conversion Efficiency. *Adv. Mater.* **2006**, *18*, 789−794.

(8) Halls, J. J. M.; Cornil, J.; dos Santos, D. A.; Silbey, R.; Hwang, D. H.; Holmes, A. B.; Bredas, J. L.; Friend, R. H. Charge- and Energy-Transfer Processes at Polymer/Polymer Interfaces: A Joint Experimental and Theoretical Study. *Phys. Rev. B* **1999**, *60*, 5721−5727.

(9) Clarke, T. M.; Ballantyne, A. M.; Tierney, S.; Heeney, M.; Duffy, W.; McCulloch, I.; Nelson, J.; Durrant, J. R. Charge Photogeneration in Low Band Gap Polyselenophene/Fullerene Blend Films. *J. Phys. Chem. C* **2010**, *114*, 8068−8075.

(10) Xu, T. T.; Qiao, Q. Q. Conjugated Polymer-Inorganic Semiconductor Hybrid Solar Cells. *Energy Environ. Sci.* **2011**, *4*, 2700−2720.

(11) Kim, B. G.; Ma, X.; Chen, C.; Ie, Y.; Coir, E. W.; Hashemi, H.; Aso, Y.; Green, P. F.; Kieffer, J.; Kim, J. Energy Level Modulation of Homo, Lumo, and Band-Gap in Conjugated Polymers for Organic Photovoltaic Applications. *Adv. Funct. Mater.* **2013**, *23*, 439−445.

(12) Berhe, S. A.; Zhou, J. Y.; Haynes, K. M.; Rodriguez, M. T.; Youngblood, W. J. Electron Transport in Acceptor-Sensitized Polymer-Oxide Solar Cells: The Importance of Surface Dipoles and Electron Cascade Effects. *ACS Appl. Mater. Interfaces* **2012**, *4*, 2955−2963.

(13) Ashcroft, M. Inhomogenous Semiconductors. In *Solid State Physics*; Brooks/Cole: Belmont, CA, 1976; pp 592−597.

(14) Jennings, P. C.; Pollet, B. G.; Johnston, R. L. Electronic Properties of Pt-Ti Nanoalloys and the Effect on Reactivity for Use in PEMFCs. *J. Phys. Chem. C* **2012**, *116*, 15241−15250.

(15) Palermo, V.; Palma, M.; Samori, P. Electronic Characterization of Organic Thin Films by Kelvin Probe Force Microscopy. *Adv. Mater.* **2006**, *18*, 145−164.

(16) Ishii, H.; Hayashi, N.; Ito, E.; Washizu, Y.; Sugi, K.; Kimura, Y.; Niwano, M.; Ouchi, Y.; Seki, K. Kelvin Probe Study of Band Bending at Organic Semiconductor/Metal Interfaces: Examination of Fermi Level Alignment. *Phys. Status Solidi A* **2004**, *201*, 1075−1094.

(17) Greiner, M. T.; Helander, M. G.; Tang, W. M.; Wang, Z. B.; Qiu, J.; Lu, Z. H. Universal Energy-Level Alignment of Molecules on Metal Oxides. *Nat. Mater.* **2012**, *11*, 76−81.

(18) Ley, L.; Smets, Y.; Pakes, C. I.; Ristein, J. Calculating the Universal Energy-Level Alignment of Organic Molecules on Metal Oxides. *Adv. Funct. Mater.* **2013**, *23*, 794−805.

(19) Braun, S.; Salaneck, W. R.; Fahlman, M. Energy-Level Alignment at Organic/Metal and Organic/Organic Interfaces. *Adv. Mater.* **2009**, *21*, 1450−1472.

(20) Davis, R. J.; Lloyd, M. T.; Ferreira, S. R.; Bruzek, M. J.; Watkins, S. E.; Lindell, L.; Sehati, P.; Fahlman, M.; Anthony, J. E.; Hsu, J. W. P. Determination of Energy Level Alignment at Interfaces of Hybrid and Organic Solar Cells under Ambient Environment. *J. Mater. Chem.* **2011**, *21*, 1721−1729.

(21) Bredas, J. L.; Street, G. B. Polarons, Bipolarons, and Solitons in Conducting Polymers. *Acc. Chem. Res.* **1985**, *18*, 309−315.

(22) While band bending typically refers to phenomenon in materials having a band structure, it is recognized that localized wave functions in organic materials do not form bands. Herein, the more general use of the term "band" is used to represent a distribution of electronic states, although the band bending phenomenon is equivalent. This is

consistent with the terminology used by the scientific community concerned with band bending in organic materials.
(23) Morris, A. J.; Meyer, G. J. TiO_2 Surface Functionalization to Control the Density of States. *J. Phys. Chem. C* **2008**, *112*, 18224−18231.
(24) Moulder, J.; Stickle, W. F.; Sobol, P. E.; Bombem, K. D. *Handbook of X-Ray Photoelectron Spectroscopy*; Physical Electronics, Inc.: Eden Prairie, MN, 1995; pp 15, 40, 121.
(25) Ishii, H.; Sugiyama, K.; Ito, E.; Seki, K. Energy Level Alignment and Interfacial Electronic Structures at Organic Metal and Organic Organic Interfaces. *Adv. Mater.* **1999**, *11*, 605−625.
(26) van Haare, J.; Havinga, E. E.; van Dongen, J. L. J.; Janssen, R. A. J.; Cornil, J.; Bredas, J. L. Redox States of Long Oligothiophenes: Two Polarons on a Single Chain. *Chem.—Eur. J.* **1998**, *4*, 1509−1522.
(27) Furukawa, Y. Electronic Absorption and Vibrational Spectroscopies of Conjugated Conducting Polymers. *J. Phys. Chem.* **1996**, *100*, 15644−15653.
(28) Yu, W. J.; Zhou, J. W.; Bragg, A. E. Exciton Conformational Dynamics of Poly(3-Hexylthiophene) (P3HT) in Solution from Time-Resolved Resonant-Raman Spectroscopy. *J. Phys. Chem. Lett.* **2012**, *3*, 1321−1328.
(29) Santos, M. J. L.; Brolo, A. G.; Girotto, E. M. Study of Polaron and Bipolaron States in Polypyrrole by in Situ Raman Spectroelectrochemistry. *Electrochim. Acta* **2007**, *52*, 6141−6145.
(30) Salvador, P.; Hidalgo, M. G.; Zaban, A.; Bisquert, J. Illumination Intensity Dependence of the Photovoltage in Nanostructured TiO_2 Dye-Sensitized Solar Cells. *J. Phys. Chem. B* **2005**, *109*, 15915−15926.
(31) Di Valentin, C.; Pacchioni, G.; Selloni, A. Reduced and N-Type Doped TiO_2: Nature of Ti^{3+} Species. *J. Phys. Chem. C* **2009**, *113*, 20543−20552.
(32) Nowotny, M. K.; Bak, T.; Nowotny, J. Electrical Properties and Defect Chemistry of TiO_2 Single Crystal. I. Electrical Conductivity. *J. Phys. Chem. B* **2006**, *110*, 16270−16282.
(33) Abdou, M. S. A.; Orfino, F. P.; Son, Y.; Holdcroft, S. Interaction of Oxygen with Conjugated Polymers: Charge Transfer Complex Formation with Poly(3-Alkylthiophenes). *J. Am. Chem. Soc.* **1997**, *119*, 4518−4524.
(34) Sperlich, A.; Kraus, H.; Deibel, C.; Blok, H.; Schmidt, J.; Dyakonov, V. Reversible and Irreversible Interactions of Poly(3-Hexylthiophene) with Oxygen Studied by Spin-Sensitive Methods. *J. Phys. Chem. B* **2011**, *115*, 13513−13518.
(35) Abdou, M. S. A.; Holdcroft, S. Mechanisms of Photodegradation of Poly(3-Alkylthiophenes) in Solution. *Macromolecules* **1993**, *26*, 2954−2962.
(36) Hintz, H.; Peisert, H.; Egelhaaf, H. J.; Chasse, T. Reversible and Irreversible Light-Induced P-Doping of P3HT by Oxygen Studied by Photoelectron Spectroscopy (XPS/UPS). *J. Phys. Chem. C* **2011**, *115*, 13373−13376.
(37) Cahen, D.; Kahn, A. Electron Energetics at Surfaces and Interfaces: Concepts and Experiments. *Adv. Mater.* **2003**, *15*, 271−277.
(38) Tengstedt, C.; Osikowicz, W.; Salaneck, W. R.; Parker, I. D.; Hsu, C. H.; Fahlman, M. Fermi-Level Pinning at Conjugated Polymer Interfaces. *Appl. Phys. Lett.* **2006**, 88.
(39) Markus, T. Z.; Itzhakov, S.; Akotzer, Y. I.; Cahen, D.; Hodes, G.; Oron, D.; Naaman, R. Energetics of CdSe Quantum Dots Adsorbed on TiO_2. *J. Phys. Chem. C* **2011**, *115*, 13236−13241.
(40) Liu, Y. X.; Scully, S. R.; McGehee, M. D.; Liu, J. S.; Luscombe, C. K.; Frechet, J. M. J.; Shaheen, S. E.; Ginley, D. S. Dependence of Band Offset and Open-Circuit Voltage on the Interfacial Interaction between TiO_2 and Carboxylated Polythiophenes. *J. Phys. Chem. B* **2006**, *110*, 3257−3261.
(41) Agarwala, S.; Kevin, M.; Wong, A. S. W.; Peh, C. K. N.; Thavasi, V.; Ho, G. W. Mesophase Ordering of TiO_2 Film with High Surface Area and Strong Light Harvesting for Dye-Sensitized Solar Cell. *ACS Appl. Mater. Interfaces* **2010**, *2*, 1844−1850.
(42) Fitzmaurice, D. Using Spectroscopy to Probe the Band Energetics of Transparent Nanocrystalline Semiconductor-Films. *Sol. Energy Mater. Sol. Cells* **1994**, *32*, 289−305.
(43) Ondersma, J. W.; Hamann, T. W. Conduction Band Energy Determination by Variable Temperature Spectroelectrochemistry. *Energy Environ. Sci.* **2012**, *5*, 9476−9480.
(44) Curran, J. S.; Lamouche, D. Transport and Kinetics in Photoelectrolysis by Semiconductor Particles in Suspension. *J. Phys. Chem.* **1983**, *87*, 5405−5411.
(45) Albery, W. J.; Bartlett, P. N. The Transport and Kinetics of Photogenerated Carriers in Colloidal Semiconductor Electrode Particles. *J. Electrochem. Soc.* **1984**, *131*, 315−325.
(46) Emeline, A. V.; Ryabchuk, V. K.; Serpone, N. Spectral Dependencies of the Quantum Yield of Photochemical Processes on the Surface of Nano-/Microparticulates of Wide-Band-Gap Metal Oxides. 1. Theoretical Approach. *J. Phys. Chem. B* **1999**, *103*, 1316−1324.
(47) Kytin, V.; Dittrich, T.; Bisquert, J.; Lebedev, E. A.; Koch, F. Limitation of the Mobility of Charge Carriers in a Nanoscaled Heterogeneous System by Dynamical Coulomb Screening. *Phys. Rev. B* **2003**, *68*, 195308.
(48) Law, M.; Greene, L. E.; Johnson, J. C.; Saykally, R.; Yang, P. D. Nanowire Dye-Sensitized Solar Cells. *Nat. Mater.* **2005**, *4*, 455−459.
(49) Hagfeldt, A.; Gratzel, M. Light-Induced Redox Reactions in Nanocrystalline Systems. *Chem. Rev.* **1995**, *95*, 49−68.
(50) Hayashi, N.; Ishii, H.; Ouchi, Y.; Seki, K. Examination of Band Bending at Buckminsterfullerene (C-60)/Metal Interfaces by the Kelvin Probe Method. *J. Appl. Phys.* **2002**, *92*, 3784−3793.
(51) Huang, S. Y.; Schlichthorl, G.; Nozik, A. J.; Gratzel, M.; Frank, A. J. Charge Recombination in Dye-Sensitized Nanocrystalline TiO_2 Solar Cells. *J. Phys. Chem. B* **1997**, *101*, 2576−2582.
(52) Nazeeruddin, M. K.; Kay, A.; Rodicio, I.; Humphrybaker, R.; Muller, E.; Liska, P.; Vlachopoulos, N.; Gratzel, M. Conversion of Light to Electricity by Cis-X_2bis(2,2′-Bipyridyl-4,4′-Dicarboxylate)-Ruthenium(II) Charge-Transfer Sensitizers (X = Cl^-, Br^-, I^-, Cn^-, and Scn^-) on Nanocrystylline TiO_2 Electrodes. *J. Am. Chem. Soc.* **1993**, *115*, 6382−6390.
(53) Goh, C.; Scully, S. R.; McGehee, M. D. Effects of Molecular Interface Modification in Hybrid Organic-Inorganic Photovoltaic Cells. *J. Appl. Phys.* **2007**, *101*, 114503.
(54) Parkanyi, C., Ed. Dipole Moments of Aromatic Heterocycles. In *Theoretical Organic Chemistry*; Elsevier Science: Amsterdam, 1998; p 234.
(55) Cahen, D.; Hodes, G.; Gratzel, M.; Guillemoles, J. F.; Riess, I. Nature of Photovoltaic Action in Dye-Sensitized Solar Cells. *J. Phys. Chem. B* **2000**, *104*, 2053−2059.
(56) Ruiz, A. M.; Dezanneau, G.; Arbiol, J.; Cornet, A.; Morante, J. R. Insights into the Structural and Chemical Modifications of Nb Additive on TiO_2 Nanoparticles. *Chem. Mater.* **2004**, *16*, 862−871.
(57) Nikolay, T.; Larina, L.; Shevaleevskiy, O.; Ahn, B. T. Electronic Structure Study of Lightly Nb-Doped TiO_2 Electrode for Dye-Sensitized Solar Cells. *Energy Environ. Sci* **2011**, *4*, 1480−1486.
(58) Stengl, V.; Hougkova, V.; Bakardjieva, S.; Murafa, N.; Bezdicka, P. Niobium and Tantalum Doped Titania Particles. *J. Mater. Res.* **2010**, *25*, 2015−2024.
(59) Devi, L. G.; Murthy, B. N.; Kumar, S. G. Photocatalytic Activity of TiO_2 Doped with Zn^{2+} and V^{5+} Transition Metal Ions: Influence of Crystallite Size and Dopant Electronic Configuration on Photocatalytic Activity. *Mater. Sci. Eng., B* **2010**, *166*, 1−6.
(60) Ryno, S. M.; Lee, S. R.; Sears, J. S.; Risko, C.; Bredas, J. L. Electronic Polarization Effects Upon Charge Injection in Oligoacene Molecular Crystals: Description Via a Polarizable Force Field. *J. Phys. Chem. C* **2013**, *117*, 13853−13860.